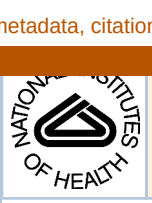

Published in final edited form as:

Drug Metab Dispos. 2008 March ; 36(3): 517–522.

The First Aspartic Acid of the DQxD Motif for Human UDP-Glucuronosyltransferase 1A10 Interacts with UDP-Glucuronic Acid during Catalysis

Yan Xiong, **Anne-Sisko Patana**, **Michael J. Miley**, **Agnieszka K. Zielinska**, **Stacie M. Bratton**, **Grover P. Miller**, **Adrian Goldman**, **Moshe Finel**, **Matt R. Redinbo**, and **Anna Radominska-Pandya**

Department of Biochemistry and Molecular Biology, University of Arkansas for Medical Sciences, Little Rock, Arkansas (Y.X., A.K.Z., S.M.B., G.P.M., A.R.-P.); Structural Biology and Biophysics, Institute of Biotechnology (A.-S.P., A.G.), and Neuroscience Center (A.G.), University of Helsinki, Helsinki, Finland; Departments of Chemistry (M.J.M.) and Biochemistry and Biophysics (M.R.R.), Program in Molecular Biology and Biotechnology (M.R.R.), and the Lineberger Comprehensive Cancer Center (M.R.R.), University of North Carolina at Chapel Hill, Chapel Hill, North Carolina; and Drug Discovery and Development Technology Center, Faculty of Pharmacy, University of Helsinki, Helsinki, Finland (M.F.)

Abstract

All UDP-glucuronosyltransferase enzymes (UGTs) share a common cofactor, UDP-glucuronic acid (UDP-GlcUA). The binding site for UDP-GlcUA is localized to the C-terminal domain of UGTs on the basis of amino acid sequence homology analysis and crystal structures of glycosyltransferases, including the C-terminal domain of human UGT2B7. We hypothesized that the ^{393}DQMD-NAK^{399} region of human UGT1A10 interacts with the glucuronic acid moiety of UDP-GlcUA. Using site-directed mutagenesis and enzymatic analysis, we demonstrated that the D393A mutation abolished the glucuronidation activity of UGT1A10 toward all substrates. The effects of the alanine mutation at Q^{394}, D^{396}, and K^{399} on glucuronidation activities were substrate-dependent. Previously, we examined the importance of these residues in UGT2B7. Although D^{393} (D^{398} in UGT2B7) is similarly critical for UDP-GlcUA binding in both enzymes, the effects of Q^{394} (Q^{399} in UGT2B7) to Ala mutation on activity were significant but different between UGT1A10 and UGT2B7. A model of the UDP-GlcUA binding site suggests that the contribution of other residues to cosubstrate binding may explain these differences between UGT1A10 and UGT2B7. We thus postulate that D^{393} is critical for the binding of glucuronic acid and that proximal residues, e.g., Q^{394} (Q^{399} in UGT2B7), play a subtle role in cosubstrate binding in UGT1A10 and UGT2B7. Hence, this study provides important new information needed for the identification and understanding of the binding sites of UGTs, a major step forward in elucidating their molecular mechanism.

UGTs metabolize many endogenous and exogenous compounds, such as bilirubin, steroids, fatty acids, bile acids, retinoids, drugs, and environmental pollutants, and, in fact, dominate phase II detoxification pathways. UGTs are highly promiscuous, catalyzing the transfer of glucuronic acid (GlcUA) from UDP-GlcUA to lipophilic substrates. The genes encoding UGTs have been assigned to two families on the basis of sequence similarities (Mackenzie et al., 1997). UGT1A isoenzymes are derived from a single gene locus; the 13 first exons encoding the N-terminal domain are unique to each isoenzyme, whereas exons 2 to 5 encoding the C-

Address correspondence to: Dr. Anna Radominska-Pandya, University of Arkansas for Medical Sciences, 4301 W. Markham, Slot 516, Little Rock, AR 72205. E-mail: radominskaanna@uams.edu.

Article, publication date, and citation information can be found at http://dmd.aspetjournals.org.

terminal domain are identical in all UGT1As (Owens and Ritter, 1992; Mackenzie et al., 1997).

UGTs belong to the GT1 family of glycosyltransferases. They are predicted to adopt a GT-B fold, which consists of two separate Rossmann-like domains with a connecting region and a catalytic site located between them (Breton et al., 2006). The C-terminal domain contains the cosubstrate binding domain, whereas the N-terminal domain contains the acceptor substrate binding site.

A full UGT crystal structure is not available. This lack of structural knowledge has resulted in the prediction of UGT structures using selective inhibitors, amino acid-specific chemical modification reagents, and amino acid alignments. Site-directed mutagenesis of the amino acids identified in those studies has been applied to the characterization of UGT binding sites with the goal of identifying critical amino acids within the binding sites (Mackenzie, 1990; Moehs et al., 1997; Senay et al., 1997; Radominska-Pandya et al., 1999; Ouzzine et al., 2000; Senay et al., 2002; Coffman et al., 2003).

Recently, progress has been made in identifying the amino acids in both the substrate and cosubstrate binding sites. Miley et al. (2007) published the 1.8-Å resolution apo crystal structure of the C-terminal domain of human UGT2B7 (2B7CT), which binds UDP-GlcUA. Comparisons of this structure with those for other members of the GT-B superfamily showed that UGT2B7 possessed a nucleotide-sugar binding site most similar to those found in the related plant flavonoid glucosyltransferases. A model of UDP-GlcUA binding to 2B7CT was used to design point mutations that would interfere with binding to different regions of UDP-GlcUA. Mutations to residues predicted to interact with the diphosphate and glucuronic acid moieties of UDP-GlcUA preferentially abolished activity, whereas mutations to residues predicted to interact with the uracil group only moderately reduced activity. In a separate study, the highly conserved His^{371} residue within the C-terminal domain of UGT1A6 was predicted to play a role in catalysis (Ouzzine et al., 2003) but was later shown to be involved in binding UDP-GlcUA along with the highly conserved Glu^{379} (Patana et al., 2007).

In the work reported here, we have used site-directed mutagenesis, modeling, and kinetic analyses to identify which amino acids in UGT1A10 are critical for UDP-GlcUA binding. We hypothesized that the ^{393}DQMDNAK^{399} amino acid sequence of UGT1A10 is the best candidate for interaction with the glucuronic acid moiety of UDP-GlcUA. We present data confirming that the DQxD motif in UGT1A10 is critical for activity. Furthermore, comparison of these results with those of similar studies we conducted with UGT2B7 suggests that there may be subtle differences between the tertiary structures and/or functions of the C-terminal domains of UGT2B7 and UGT1A10 and possibly between the 1A and 2B families as a whole.

Materials and Methods

Materials

[^{14}C]4-Nitrophenol (pNP, 6.4 mCi/mmol), saccharolactone (saccharic acid-1,4-lactone), UDP-GlcUA, and horseradish peroxidase- conjugated mouse anti-rabbit IgG were purchased from Sigma-Aldrich (St. Louis, MO). [^{14}C]UDP-GlcUA (325 mCi/mmol) was purchased from PerkinElmer Life and Analytical Sciences (Boston, MA). The His Hi-trap columns and ECL Western blotting detection system were from GE Healthcare (Piscataway, NJ). Anti-UGT1A antibody was from BD Biosciences Gentest (San Jose, CA) and the anti-tetraHis antibody was from QIAGEN (Valencia, CA). All other chemicals and solvents were of analytical grade.

Cloning and Expression of Human Recombinant His-Tagged UGTs

Details of the cloning and expression of UGT1A10 in baculovirus-infected Sf9 insect cells as His-tagged proteins and the preparation of enriched membrane fractions have been reported previously (Kurkela et al., 2003; Kuuranne et al., 2003). The same is true for human UGT2B7 cloning and expression (Miley et al., 2007)

Site-Directed Mutagenesis and Expression of Mutated Recombinant Proteins

Wild-type UGT1A10 DNA was subcloned between the BamHI and HindIII site of plasmid pcDNA3.1(+) (Invitrogen, Carlsbad, CA) to generate pcDNA-UGT1A10 for use as a template for site-directed mutagenesis. Site-directed mutagenesis was performed using the QuikChange Site-Directed Mutagenesis Kit (Stratagene, La Jolla, CA) according to the manufacturer's instructions. The mutagenic primers used, with the mutated nucleotides underlined, were D393A-for 5′-GCCCTTGTTTGGTG*CC*CAGATGGACAATG-3′, Q394A-for 5′-CCTTGTTTGGTGAT*GC*GATGGACAATGCAAAGC-3′, D396A-for 5′-GGTGATCAGATGG*CC*AATGCAAAGCGC-3′, and K399A-for 5′-CAGATGGACAATGCA*GC*GCGCATGGAGAC-3′.

These oligonucleotides and their reverse complement primer pairs were used in each reaction, and each mutagenesis was verified by DNA sequencing. Subsequently, new recombinant baculovirus was generated using the Bac-to-Bac system (Invitrogen), followed by the production of the mutant proteins in insect cells as described previously (Kurkela et al., 2003). Wild-type and mutant protein expression levels were determined by Western blot analysis using anti-UGT1A and anti-tetraHis antibodies, and the protein levels were standardized as described previously (Luukkanen et al., 2005). The details of human UGT 2B7 mutant protein expression have been reported previously (Miley et al., 2007)

Enzymatic Assays and Kinetic Analyses

We measured glucuronidation of pNP, 2-hydroxyestrone (2-OH-E1), tetrachlorocatechol (TCC), chrysin, and genistein for UGT1A10 and glucuronidation of androsterone, hyodeoxycholic acid, and TCC for UGT2B7 as described previously (Senay et al., 1999). Briefly, we used membrane protein from wild-type UGT1A10 and the D393A, Q294A, D396A, and K399A mutants and wild-type UGT2B7 and the D398A and Q399A mutants. The protein was incubated in 100 μM Tris-HCl (pH 7.4)-5 mM for $MgCl_2$-5 mM saccharolactone with each substrate (750 μM, for screening) in a total volume of 30 μl. The reactions were started by adding 4 mM of either unlabeled or [^{14}C]UDP-GlcUA and incubated at 37°C for 20 min.

Apparent kinetic values for each UGT1A10-based enzyme toward both the substrate and cosubstrate were analyzed. To determine the K_m and V_{max} values for these enzymes toward pNP, we added 100 to 4000 μM [^{14}C]pNP, started the reactions by adding 4 mM UDP-GlcUA, and then incubated them at 37°C for 20 min in a total volume of 30 μl. To determine the K_m and V_{max} values for these enzymes toward UDP-GlcUA, we used 100 to 5000 μM UDP-GlcUA, started the reactions by adding 1 mM [^{14}C]pNP, and incubated them at 37°C for 20 min in a total volume of 30 μl.

For each assay, the reactions were stopped by adding 30 μl of ethanol. Aliquots (40 μl) of each sample were then applied to the preabsorbent layer of channeled silica gel thin-layer chromatography (TLC) plates [Baker 250Si-PA (19C), VWR Scientific, Sugarland, TX], and glucuronidated products and unreacted substrates were separated by development in chloroform-methanol-glacial acetic acid-water (65:25:2:4, v/v).

Radioactive compounds were localized on TLC plates by autoradiography for 3 to 4 days at −80°C. Silica gel in areas corresponding to the glucuronide bands identified from autoradiograms and the corresponding areas from control lanes were scraped from the TLC plates into scintillation vials, and radioactivity was measured using a Perkin-Elmer liquid scintillation counter (Packard Tri-Carb 2100TR). The results of these experiments were analyzed and apparent kinetic parameters were determined using Prism 4 software (GraphPad Software Inc., San Diego, CA).

Homology Modeling

A model of part of the C-terminal domain of UGT1A10, residues 280 to 441, was built using the Homology module in the Insight II program (version 2005; Accelrys, San Diego, CA). The structure of the corresponding domain in UGT2B7 (2O6L) was used as the template. The sequences were aligned using EMBOSS pairwise alignment algorithms (http://www.ebi.ac.uk/emboss/align/). The model was minimized in the Insight II Discover module using the Amber force field. Steepest descent was used, followed by conjugate gradient minimization until 0.001 root mean square energy gradient was achieved. The quality of the model was verified by Procheck v3.5.4. The cosubstrate UDP-GlcUA was manually docked into the partial model of UGT1A10 in the same conformation as UDP-glucose in the plant flavonoid glucosyltransferase (*Vv*GT1) structure (Offen et al., 2006). The enzyme-UDP-GlcUA complex was further minimized using the Amber force field as well as steepest descent and conjugate gradient minimizations.

Results

Site-Directed Mutagenesis of UGT1A10

Several amino acids in the ^{393}DQMDNAK^{399} region of UGT1A10 are thought to be involved with UDP-GlcUA binding. Structural data suggested that D^{393} and Q^{394} make direct contact with the glucuronic acid moiety of UDP-GlcUA. In addition, D^{396} is highly conserved among UGT enzymes, although it is not predicted to interact directly with the UDP-GlcUA cosubstrate. Lastly, the solvent-exposed K^{399} residue could play a secondary role in ligand binding. To begin to assess the roles of these residues, we constructed four recombinant UGT1A10 mutants: D393A, Q394A, D396A, and K399A. Wild-type and mutant protein expression levels were determined by Western blot analysis using anti-UGT1A and anti-tetraHis antibodies, and all proteins were expressed in sufficient amounts (data not shown).

Analysis of Recombinant Protein Activity

Wild-type UGT1A10, D393A, Q394A, D396A, and K399A were assayed for activity toward several prototypical UGT1A10 substrates, and the glucuronidation products were separated by TLC (Fig. 1). Replacing D^{393} with alanine totally abolished the activity of this protein toward all of the substrates under investigation. However, the other three mutants, Q394A, D396A, and K399A, were all partially active. They all showed wild-type activity with TCC as a substrate but varying activity with all of the other substrates (Fig. 1). D396A was much less active with pNP and 2-OH-E1 but showed wild-type activity with the flavonoid substrates, chrysin and genistein. There was a significant decrease in the activity of Q394A toward these four substrates, with nearly complete inactivity toward pNP. K399A showed no change in activity toward pNP or 2-OH-E1 compared with the wild type, but it was significantly less active with genistein, and, interestingly, significantly more active with chrysin.

Kinetic Analysis of Wild-Type UGT1A10 and Mutant Enzymes toward pNP and UDP-GlcUA

The apparent kinetic parameters for the D393A and Q394A mutants with pNP could not be calculated because they were inactive toward this substrate. For D396A with pNP as substrate,

the $K_{m\ (pNP)}$ value was unchanged from that of the wild type, but the $V_{max\ (pNP)}$ decreased approximately 3-fold (Table 1; Fig. 2). The K399A mutant kinetics changed more with pNP, i.e., the apparent $K_{m\ (pNP)}$ and $V_{max\ (pNP)}$ values increased ~3- and 5-fold, respectively.

We determined the kinetic parameters toward UDP-GlcUA for wild-type UGT1A10 and mutants D396A and K399A at constant pNP concentrations (Table 1; Fig. 2). The $K_{m\ (UDP\text{-}GlcUA)}$ values for both D396A and K399A increased approximately 1.5-fold compared with the wild type. However, the $V_{max\ (UDP\text{-}GlcUA)}$ value for D396A was essentially unchanged, whereas the $V_{max\ (UDP\text{-}GlcUA)}$ increased 3-fold.

Comparison of the Effects of the D393A and Q394A Mutations on UGT1A10 and UGT2B7 Activity

Figure 3 juxtaposes the effect of D393A and Q394A on UGT1A10 activity to the effect of the corresponding mutations, D398A and Q399A, on UGT2B7 glucuronidation of typical UGT1A10 and UGT2B7 substrates. The Asp→Ala mutation totally abolished the catalytic activity in UGT1A10 and severely impaired the activity in UGT2B7, but the Gln→Ala mutation affected the two isoenzymes differently. In UGT2B7, the Q399A mutation resulted in total loss of activity, whereas in UGT1A10, the effect was substrate-dependent; only activity toward pNP was abolished.

Homology Modeling

To shed new light on UDP-GlcUA binding in general and on the apparent differences between UGT1A10 and UGT2B7 in particular, a model of UDP-GlcUA bound to UGT1A10 and UGT2B7 (Fig. 4) was built. The structure of the UDP-GlcUA binding fragment of UGT2B7 (Miley et al., 2007) was used as a template to generate a model of the C-terminal domain of UGT1A10. However, because the UGT2B7 structure does not have cosubstrate bound, we manually docked UDP-GlcUA to the UGT1A10 partial model in the same conformation as UDP-glucose in *Vv*GT1 (Offen et al., 2006). The docking shows how H^{369}, E^{378}, D^{393}, and Q^{394} (UGT1A10 numbering) are arranged around the UDP-GlcUA. All of these residues have been implicated in UDP-GlcUA binding in UGT1A10 (this study), UGT2B7 (Miley et al., 2007), or UGT1A6 (Patana et al., 2007). Furthermore, S^{372} and H^{373} (UGT1A10 numbering) also appear to be important on the basis of the docked model. These two residues, which are not identical in all UGTs (Figs. 4 and 5), can hydrogen bond to the UDP-GlcUA; the changes at these residues may thus explain some of the differences in UDP-GlcUA binding between UGT1A10 and UGT2B7, as S^{372} is replaced by Ala and H^{373} by Asn in UGT2B7, respectively.

Discussion

The present studies were undertaken to clarify the role of D^{393}, Q^{394}, D^{396}, and K^{399} in the binding of UDP-GlcUA and the catalytic activity of UGT1A10. Of the four mutated residues, D^{393} is apparently essential for binding UDP-GlcUA because of the complete loss of activity in the D393A mutant. In contrast, D^{396} plays a minor role in substrate turnover, but the 1.5-fold decrease in $K_{m\ (UDP\text{-}GlcUA)}$ indicates a weaker association for the cosubstrate. This alteration in cosubstrate binding compromises pNP turnover, as shown by a 3-fold decrease in $V_{max\ (pNP)}$ without any change $K_{m\ (pNP)}$.

The conserved K^{399} also might have a role in cosubstrate binding. Surprisingly, the K399A mutant led to significant reorganization of the Michaelis complex; there were changes in V_{max} and K_m for both substrate and cofactor. Even though $K_{m\ (pNP)}$ increased 3-fold, $V_{max\ (pNP)}$ increased 5-fold, leading to an almost 2-fold increase in efficiency as measured by V_{max}/K_m. Similarly, $K_{m\ (UDP\text{-}GlcUA)}$ increased 1.5-fold, whereas $V_{max\ (UDP\text{-}GlcUA)}$ increased 3-fold, with the net effect being a 2-fold increase in catalytic efficiency. Although the effect

on K_m suggests changes in recognition of substrate and cosubstrate, the effect on V_{max} supports changes in the rate-limiting step(s) that depend on interactions with both molecules.

Although the molecular details of the catalytic cycle are not known for this reaction, we speculate that K^{399} coordinates substrate and cofactor indirectly to form the Michaelis complex and may also be involved with releasing coupled product. Because the coupled product contains both substrate and most of the cofactor, weaker binding of the individual molecules would be additive, and the mutant would bind product more weakly than the wild type. If product release is rate-limiting, the increase in V_{max} may be due to decreased affinity of the mutant for product. Taken together, these studies suggest that K^{399} plays a role in coordinating interactions between substrate and cofactor to elicit catalytic turnover. The higher efficiency of the mutant reflects the ability to saturate the enzyme to maximize turnover. However, within a cell, the high K_m values for substrate and cofactor may preclude saturation of the enzyme, leading to less efficient turnover. Further analysis of the catalytic role of K^{399} is clearly warranted.

The novelty of the role of D^{393} in UGT1A10 activity has broader implications because of the conservation of this residue in all human UGTs (Fig. 5). Comparison of the apo structure of the C-terminal domain of human UGT2B7 (2B7CT) (Miley et al., 2007) with those of *Vv*GT1 and UGT71G1 from the plant *Medicago truncatula* revealed a high level of structural homology despite their low sequence identity (~19%). Because 2B7CT only crystallized in the absence of UDP-GlcUA, it was modeled into the 2B7CT structure using the structure of *Vv*GT1 as a guide. On the basis of this model, the residues of UDP-GlcUA binding were classified into three groups: residues predicted to interact with the glucuronic acid, uracil base, and diphosphate moieties, respectively (Fig. 6). A panel of point mutations at those positions was generated, and their impact on UGT2B7 enzyme activity was investigated (Miley et al., 2007).

The analysis of UGT2B7 motif substitutions demonstrates changes in catalytic parameters similar to those observed for UGT1A10 (Fig. 3) (Miley et al., 2007). The UGT2B7 residues targeted in that study (D^{398} and Q^{399}) correspond to D^{393} and Q^{394} in the DQxDxxK motif in UGT1A10. An alanine at either of these positions severely compromises enzyme activity (Miley et al., 2007), although the specific effects on the kinetic parameters were not determined. An important difference between these UGTs is the magnitude of the effects on the respective enzymatic activities. Although the D393A UGT1A10 mutant is completely inactive, the D398A UGT2B7 mutant retains residual activity. Conversely, the Q394A UGT1A10 mutant retains activity, although with significant variability depending on substrate; the corresponding Q399A UGT2B7 mutant is inactive. There might therefore be differences between the tertiary structures and functions of the C-terminal domains of UGT2B7 and UGT1A10 and possibly between the UGT1A and UGT2B families as a whole. This difference is not surprising when the relatively low amino acid sequence homology between these enzymes in this region (51% in the region shown in Fig. 5) is taken into account.

Why should the D→A and Q→A substitutions have different effects in UGT1A10 and UGT2B7 even though the motif is conserved? We explain this observation through our homology model of the UDP-GlcUA binding site for UGT1A10 based on the UGT2B7 partial structure. In the superimposed structures, not only do D^{393} and Q^{394} (UGT1A10 numbering) occupy approximately the same position but also the UGT1A10/UGT2B7 residues H^{369}/H^{374}, E^{377}/E^{382}, D^{393}/D^{398}, and Q^{394}/Q^{399} adopt similar positions in the binding site. Nevertheless, the structures display different hydrogen bonding patterns. At the bottom of the binding site in Fig. 4, UGT1A10 and UGT2B7 do not use the same residues to coordinate UDP-GlcUA. Specifically, UGT1A10 uses S^{372} and H^{373} for binding, whereas UGT2B7 uses A^{377} and N^{378}. Hydrogen bonding between S^{372} and the sugar moiety of UDP-GlcUA in UGT1A10 is not possible for UGT2B7. This change may explain the more severe effect of the

Glu→Ala substitution in UGT2B7 compared with that of UGT1A10. The Q394A mutant of UGT1A10 may retain partial activity because of the stabilizing hydrogen bond through S^{372}. The presence of H^{373} (N^{378} in UGT2B7) may also induce a less obvious effect on substrate turnover. The other two residues of UGT1A10 studied, D^{396} and K^{399}, do not appear to interact with the cosubstrate directly.

In summary, these results suggest that UDP-GlcUA interacts with D^{393} and that mutation of this amino acid results in the total loss of enzyme activity. In addition, the identification of this specific amino acid as having a critical role in UDP-GlcUA binding can be extrapolated to all UGTs, as evidenced by crystal structure data (Miley et al., 2007). In the future, this knowledge could be exploited for the design of UDP-GlcUA analogs of clinical and pharmacological importance with the aim of increasing and/or decreasing the biological response of UGTs and/or eliminating any undesired side effects of glucuronidation.

Acknowledgements

The authors acknowledge the efforts of Joanna Little in the skillful editing of this manuscript and thank Anna Gallus-Zawada, Johanna Mosorin, Kaisa Laajanen, and Nina Sneitz for technical assistance.

This work was supported in part by National Institutes of Health (NIH) Grants DK56226, DK60109, and GM075893 (A.R.-P.). A.R.-P. is also supported by tobacco settlement funds from the University of Arkansas for Medical Sciences. The work in Helsinki was supported by grants from the Academy of Finland [Projects 207535 (M.F.) and 1105157 and 1114752 (A.G.)] and the Sigrid Jusélius Foundation (M.F. and A.G.) and by Biocentrum Helsinki (A.G.). The work at University of North Caroline was supported in part by NIH Grant CA98468 (M.R.R.)

References

Breton C, Snajdrova L, Jeanneau C, Koca J, Imberty A. Structures and mechanisms of glycosyltransferases. Glycobiology 2006;16:29R–37R. [PubMed: 16049187]

Coffman BL, Kearney WR, Goldsmith S, Knosp BM, Tephly TR. Opioids bind to the amino acids 84 to 118 of UDP-glucuronosyltransferase UGT2B7. Mol Pharmacol 2003;63:283–288. [PubMed: 12527799]

Kurkela M, Garcia-Horsman JA, Luukkanen L, Morsky S, Taskinen J, Baumann M, Kostiainen R, Hirvonen J, Finel M. Expression and characterization of recombinant human UDP-glucuronosyltransferases (UGTs): UGT1A9 is more resistant to detergent inhibition than other UGTs and was purified as an active dimeric enzyme. J Biol Chem 2003;278:3536–3544. [PubMed: 12435745]

Kuuranne T, Kurkela M, Thevis M, Schanzer W, Finel M, Kostiainen R. Glucuronidation of anabolic androgenic steroids by recombinant human UDP-glucuronosyltransferases. Drug Metab Dispos 2003;31:1117–1124. [PubMed: 12920167]

Luukkanen L, Taskinen J, Kurkela M, Kostiainen R, Hirvonen J, Finel M. Kinetic characterization of the 1A subfamily of recombinant human UDP-glucuronosyltransferases. Drug Metab Dispos 2005;33:1017–1026. [PubMed: 15802387]

Mackenzie PI. Expression of chimeric cDNAs in cell culture defines a region of UDP glucuronosyltransferase involved in substrate selection. J Biol Chem 1990;265:3432–3435. [PubMed: 2105949]

Mackenzie PI, Owens IS, Burchell B, Bock KW, Bairoch A, Belanger A, Fournel-Gigleux S, Green M, Hum DW, Iyanagi T, et al. The UDP glycosyltransferase gene superfamily: recommended nomenclature update based on evolutionary divergence. Pharmacogenetics 1997;7:255–269. [PubMed: 9295054]

Miley M, Zielinska A, Keenan J, Bratton S, Radominska-Pandya A, Redinbo M. Crystal structure of the cofactor-binding domain of the human phase II drug-metabolism enzyme UDP-glucuronosyltransferase 2B7. J Mol Biol 2007;369:498–511. [PubMed: 17442341]

Moehs CP, Allen PV, Friedman M, Belknap WR. Cloning and expression of solanidine UDP-glucose glucosyltransferase from potato. Plant J 1997;11:227–236. [PubMed: 9076990]

Offen W, Martinez-Fleites C, Yang M, Kiat-Lim E, Davis BG, Tarling CA, Ford CM, Bowles DJ, Davies GJ. Structure of a flavonoid glucosyltransferase reveals the basis for plant natural product modification. EMBO J 2006;25:1396–1405. [PubMed: 16482224]

Ouzzine M, Antonio L, Burchell B, Netter P, Fournel-Gigleux S, Magdalou J. Importance of histidine residues for the function of the human liver UDP-glucuronosyltransferase UGT1A6: evidence for the catalytic role of histidine 370. Mol Pharmacol 2000;58:1609–1615. [PubMed: 11093802]

Ouzzine M, Barre L, Netter P, Magdalou J, Fournel-Gigleux S. The human UDP-glucuronosyltransferases: structural aspects and drug glucuronidation. Drug Metab Rev 2003;35:287–303. [PubMed: 14705862]

Owens IS, Ritter JK. The novel bilirubin/phenol UDP-glucuronosyltransferase UGT1 gene locus: implications for multiple nonhemolytic familial hyperbilirubinemia phenotypes. Pharmacogenetics 1992;2:93–108. [PubMed: 1306114]

Patana AS, Kurkela M, Goldman A, Finel M. The human UDP-glucuronosyltransferase: identification of key residues within the nucleotide-sugar binding site. Mol Pharmacol 2007;72:604–611. [PubMed: 17578897]

Radominska-Pandya A, Czernik PJ, Little JM, Battaglia E, Mackenzie PI. Structural and functional studies of UDP-glucuronosyltransferases. Drug Metab Rev 1999;31:817–899. [PubMed: 10575553]

Senay C, Battaglia E, Chen G, Breton R, Fournel-Gigleux S, Magdalou J, Radominska-Pandya A. Photoaffinity labeling of the aglycon binding site of the recombinant human liver UDP-glucuronosyltransferase UGT1A6 with 7-azido-4-methylcoumarin. Arch Biochem Biophys 1999;368:75–84. [PubMed: 10415114]

Senay C, Jedlitschky G, Terrier N, Burchell B, Magdalou J, Fournel-Gigleux S. The importance of cysteine 126 in the human liver UDP-glucuronosyltransferase UGT1A6. Biochim Biophys Acta 2002;1597:90–96. [PubMed: 12009407]

Senay C, Ouzzine M, Battaglia E, Pless D, Cano V, Burchell B, Radominska A, Magdalou J, Fournel-Gigleux S. Arginine 52 and histidine 54 located in a conserved amino-terminal hydrophobic region (LX2–R52-G-H54–X3-V-L) are important amino acids for the functional and structural integrity of the human liver UDP-glucuronosyltransferase UGT1*6. Mol Pharmacol 1997;51:406–413. [PubMed: 9058595]

ABBREVIATIONS

UGT
: UDP-glucuronosyltransferase

UDP-GlcUA
: UDP-glucuronic acid

pNP
: *p*-nitrophenol

2-OH-E1
: 2-hydroxyestrone

TCC
: tetrachlorocatechol

TLC
: thin-layer chromatography

***Vv*GT1**
: plant UDP-glucose:flavonoid 3-*O*-glycosyltransferase

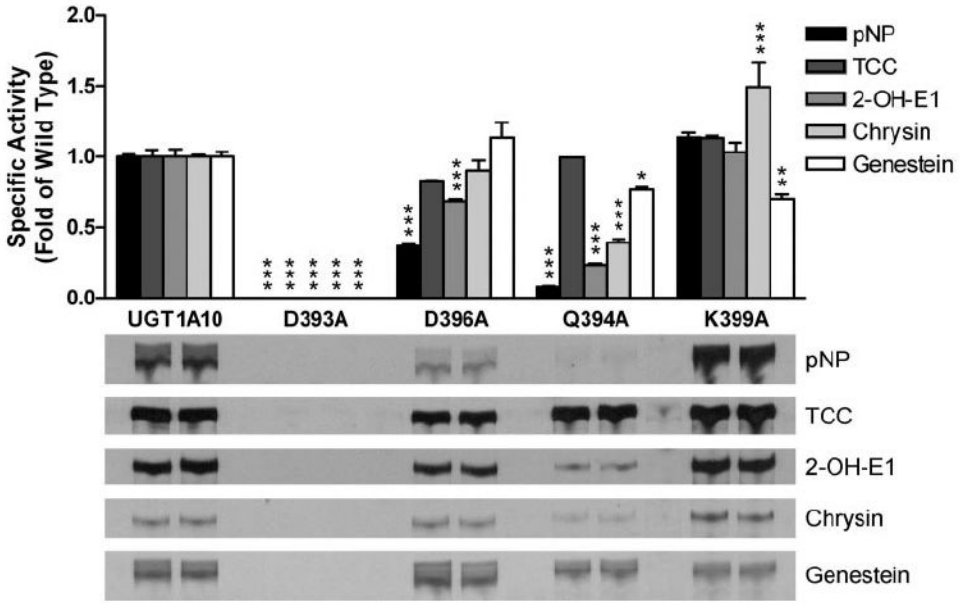

FIG. 1.

Screening of the glucuronidation of pNP, 2-OH-E1, TCC, chrysin, and genistein by recombinant human UGT1A10 and mutants D396A, Q394A, D393A, and K399A. Glucuronidation activity was measured using membrane fractions of recombinant wild-type and mutant UGTs expressed as His-tagged proteins in baculovirus-infected Sf9 insect cells. Products were separated by TLC and identified by autoradiography as described under *Materials and Methods*. The results were analyzed by one-way analysis of variance followed by a Dunnett's multiple comparison test. Measurements that vary significantly from the dimethyl sulfoxide control are indicated. *, $p < 0.05$; **, $p < 0.01$; ***, $p < 0.001$).

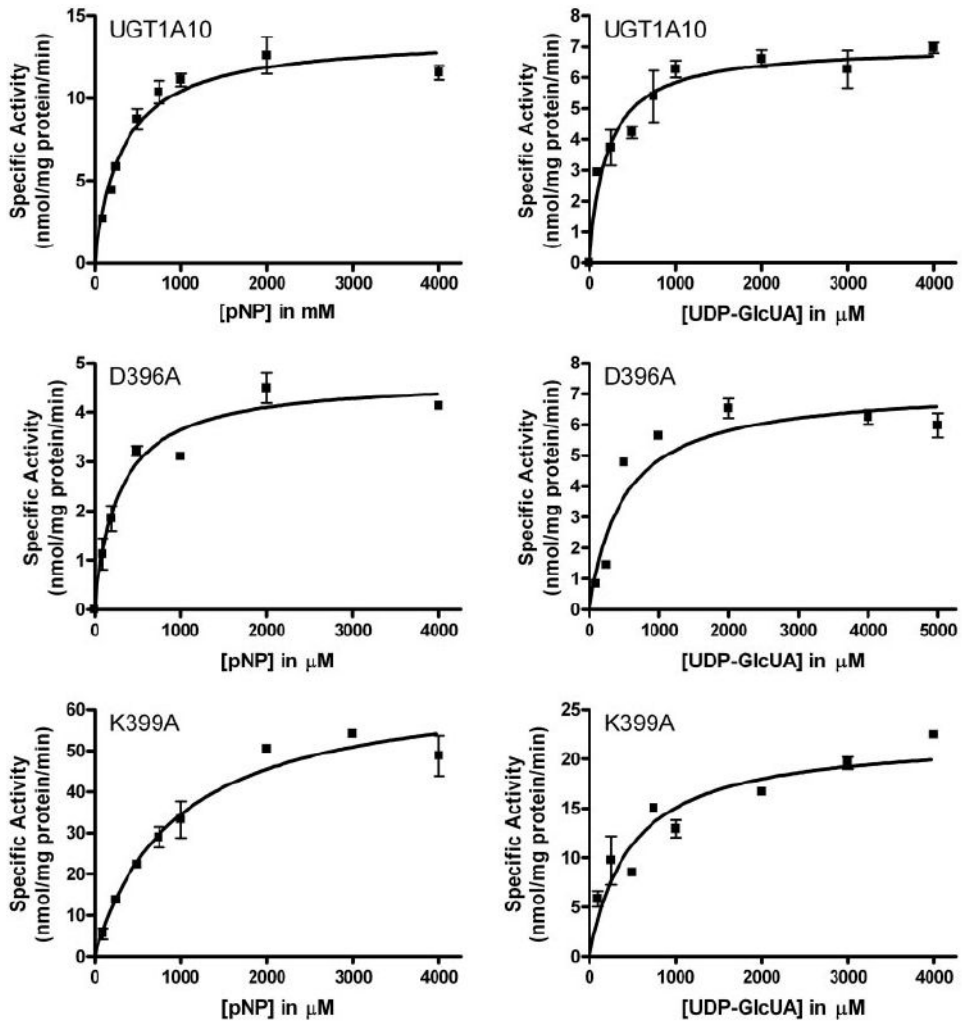

FIG. 2.

Determination of kinetic parameters for glucuronidation of pNP and binding of UDP-GlcUA by recombinant UGT1A10 and mutants D393A, Q394A, D393A, and K399A. Assays were carried out by incubating membrane fractions containing recombinant UGT1A10 (10 μg) or its mutants (20 μg) with increasing concentrations (shown in the figure) of pNP at a constant concentration of [^{14}C]UDP-GlcUA (4 mM), or with increasing concentrations (shown in the figure) of UDP-GlcUA at a constant concentration of [^{14}C]pNP (1 mM) for 20 min at 37°C. These were used to obtain apparent kinetic parameters with pNP and UDP-GlcUA, respectively. Reactions were stopped by the addition of ethanol, and products separated by TLC and identified by autoradiography as described under *Materials and Methods*. Curve fits were determined using GraphPad Prism 4 software. The curve fits to the data from each of the substrates (mean ± S.E.M. of two to four determinations) are shown.

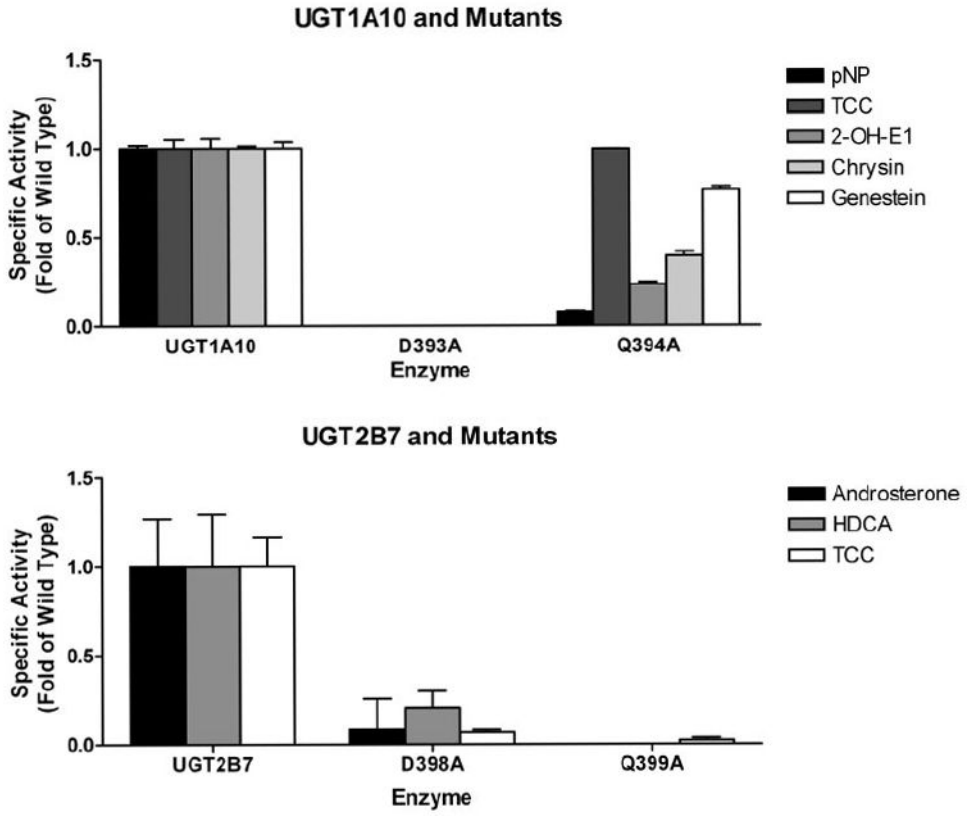

FIG. 3.

Comparison of the effects of DQ mutation on UGT1A10 and UGT2B7. Glucuronidation activity was measured using membrane fractions of recombinant UGTs expressed as His-tagged proteins in baculo-virus-infected Sf9 insect cells using typical UGT1A10 and UGT2B7 substrates.

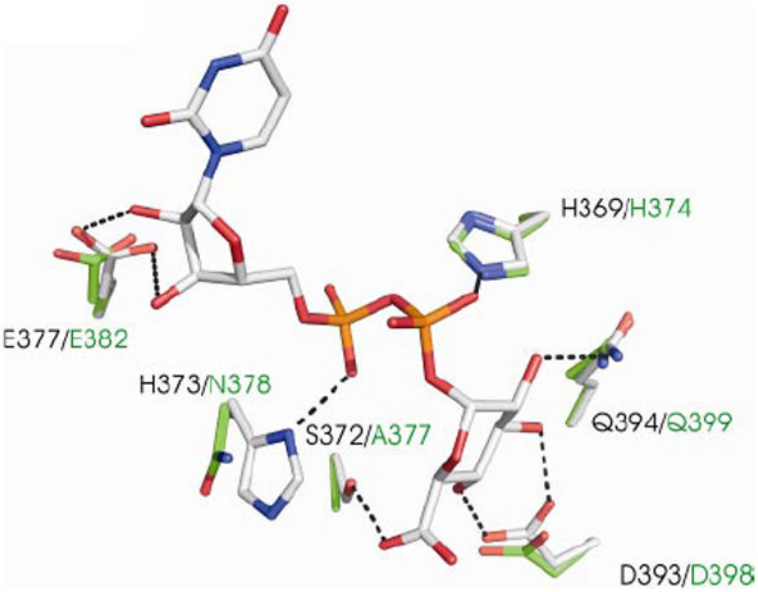

FIG. 4.

A ball-and- stick representation of the model of the UDP-GlcUA binding site in UGT1A10 (carbon, gray) and UGT2B7 (carbon, green). (In both models: blue, nitrogen; red, oxygen; and orange, phosphate.) Dashed black lines represent possible hydrogen bonds. A model of the UDP-GlcUA binding site of UGT1A10 was built using the structure of this domain in UGT2B7 as a template (see *Materials and Methods* for details). The figure (produced in PyMOL [http://www.pymol.org]) shows the bound cosubstrate and the location of key residues in either UGT1A10 or UGT2B7 within the hydrogen-bonding distance. The residue types and numbering are indicated for both UGT1A10 (black) and UGT2B7 (green).

FIG. 5.

Amino acid sequence alignment. Amino acid sequence alignment of UGT1A, UGT2B4, UGT2B7, UGT2B10, UGT2B11, UGT2B15, UGT2B17, 2-hydroxyacylsphingosine 1-*β*-galactosyl-transferase (CGT), baculovirus ecdysteroid UDP-glucosyltransferase (BeGT), *Streptomyces lividans* macrolide glycosyltransferase (MGT), and *Escherichia vulneris* zeaxanthin glucosyltransferase (CRTX). Numbers related to the amino acid sequences are based on information deposited in GenBank (UGT1A1: AF180372; UGT2B4: NP 066962; UGT2B7: NP 001065; UGT2B10: NP 001066; UGT2B11: NP 001064; UGT2B15: NP 001067; UGT2B17: NP 001068; CGT: JC5423; BeGT: AAA66785; MGT: ABA28305; and CRTX: Q01330). *, numbering is based on UGT1A1 (for UGT1A3, 1A4, and 1A5, add 1; for UGT1A6 subtract 1; for UGT1A7, 1A8, 1A9, and 1A10 subtract 2). ■, amino acids conserved in all aligned enzymes; ♦, amino acids conserved in all but one aligned enzyme.

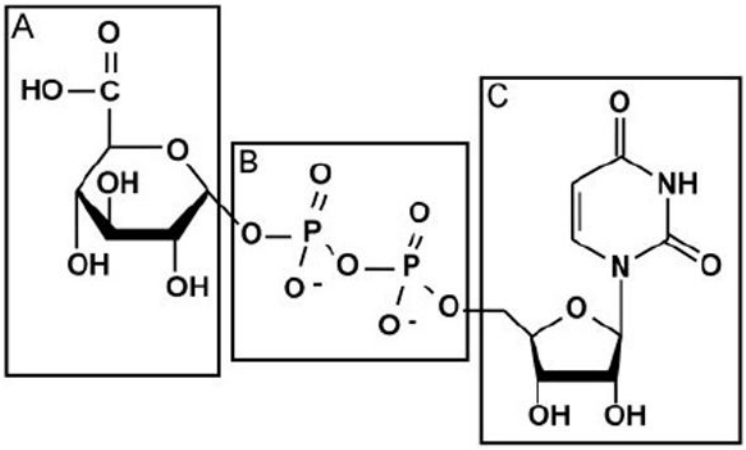

FIG. 6.
UDP-GlcUA moieties. The structure of UDP-GlcUA contains glucuronic acid (A), diphosphate (B), and nucleic acid moieties (C), all of which could interact with amino acids in the UGT structure.

TABLE 1

Steady-state parameters for pNP glucuronidation by substituted UGT1A10 enzymes

Parameters were determined from the fit of initial velocities to a Michaelis-Menten kinetic scheme using the software GraphPad Prism.

UGT Isoform	pNP			UDP-GlcUA		
	V_{max}	K_m	V_{max}/K_m	V_{max}	K_m	V_{max}/K_m
	μM min^{-1} mg^{-1} protein	*μM*	*min^{-1} mg^{-1} protein*	*μM min^{-1} mg^{-1} protein*	*μM*	*min^{-1} mg^{-1} protein*
1A10 WT	13.8 ± 0.6	323 ± 54	0.043 ± 0.007	7.0 ± 0.3	323 ± 54	0.022 ± 0.004
D393A						
Q394A						
D396A	4.7 ± 0.2	286 ± 56	0.016 ± 0.003	7.2 ± 0.6	490 ± 150	0.015 ± 0.004
K399A	67 ± 5	940 ± 170	0.071 ± 0.013	22 ± 2	480 ± 140	0.046 ± 0.013

WT, wild type.